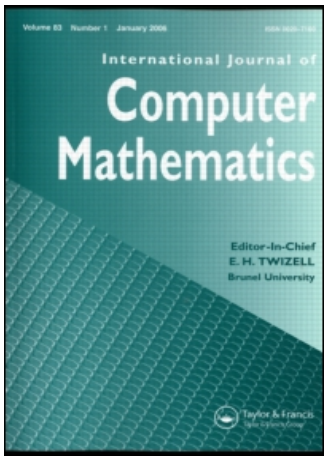


International Journal of Computer Mathematics
Publication details, including instructions for authors and subscription information:
http://www.informaworld.com/smpp/title~content=t713455451

# Operator splitting techniques for the numerical analysis of natural convection heat transfer

Online Publication Date: 01 June 2007
To cite this Article: Ilicak, Mehmet, Ecder, Ali and Turan, Erhan , (2007) 'Operator splitting techniques for the numerical analysis of natural convection heat transfer', International Journal of Computer Mathematics, 84:6, 783 - 793
To link to this article: DOI: 10.1080/00207160701458278
URL: http://dx.doi.org/10.1080/00207160701458278

*International Journal of Computer Mathematics*
Vol. 84, No. 6, June 2007, 783–793

Taylor & Francis
Taylor & Francis Group

# Operator splitting techniques for the numerical analysis of natural convection heat transfer

MEHMET ILICAK, ALI ECDER* and ERHAN TURAN

Department of Mechanical Engineering, Bogazici University Bebek, Istanbul 34342, Turkey

*(Received 19 July 2006; revised version received 15 January 2007; accepted 18 January 2007)*

Natural convection heat transfer in rectangular enclosures is an active research area, due to its significance for both fundamental interest and engineering applications such as thermal management of electronic components. In this present numerical study, combined conduction and natural convection have been analysed for one or two heat sources mounted on substrates in an enclosure. For one heat source, the substrate is mounted on a vertical wall, and for the case of two heat sources, the substrates are mounted vertically and horizontally. Buoyancy forces drive the fluid flow. The Picard method with a hybrid grid system is utilized to decouple between pressure and velocity components, resulting in componentwise splitting. Linear systems obtained via the Picard method have been solved by the ADI method, resulting in directional splitting. Effects of different parameters such as Prandtl number, Rayleigh number, and boundary conditions on the temperature and flow field have been analysed.

*Keywords*: Operator splitting; Componentwise splitting; Directional splitting

*AMS Subject Classifications*: 65N99; 65F10

## 1. Introduction

The increased power dissipation of today's integrated circuits has made the understanding of thermal constraints important to those who manufacture and use these devices. In industrial applications, if heat dissipation systems are implemented untested, developed strictly by trial-and-error, server systems may fail due to heat build-up and component wear. As the density of circuits increases, so does the need to develop effective methods of thermal management and packaging [1–7].

Although radiation has an important role in the heat transfer inside an enclosure, the major heat transfer mode is convection. In addition, enclosure boundary conditions, including the location and orientation of the substrate on which the heat source is located, affect the temperature field significantly.

Madhavan and Sastri [8] conducted a parametric study considering natural convection cooling of a heat source mounted on a substrate vertically within an enclosure, neglecting radiation. They investigated the significance of different dimensionless parameters like Prandtl,

*Corresponding author. Email: ecder@boun.edu.tr

*International Journal of Computer Mathematics*
ISSN 0020-7160 print/ISSN 1029-0265 online © 2007 Taylor & Francis
http://www.tandf.co.uk/journals
DOI: 10.1080/00207160701458278

Rayleigh and Nusselt numbers, and discussed possible choices for the enclosure boundary conditions. They utilized a nonstaggered grid structure, and with the help of a power-law scheme, they determined the velocity values on the faces of their finite-volume cells. The SIMPLEC algorithm was used to resolve the coupling between velocities and pressure appearing in the governing equations. A direct method, Gauss Elimination, was used to solve the resulting tridiagonal matrices. They stated that Rayleigh number, Prandtl number and enclosure boundary conditions strongly affect the fluid flow and heat transfer characteristics.

Sezai and Mohamad [9] studied natural convection heat transfer due to a discrete heat source on the bottom of an enclosure. Navier–Stokes equations are solved by using a multigrid technique applied to three-dimensional staggered grids discretized with the help of the finite volume method and a third-order QUICK scheme. They studied the effects of Rayleigh number, chip aspect ratio and sidewall boundary conditions on the rate of heat transfer.

Dağtekin and Öztop [10] conducted a numerical study considering heat transfer and fluid flow of two heated vertical plates within an enclosure. The algebraic equations, obtained from transport equations with the help of finite volume discretization, were solved using a line-by-line TDMA with the SIMPLEM algorithm. For convective terms a power-law difference scheme, and for diffusion terms a central difference scheme were used, as recommended, for this algorithm. They found that the position of heat sources significantly affected the flow field.

Numerical solutions to the full Navier–Stokes equations usually require considerable computer memory and computational speed. Many numerical simulations of Navier–Stokes equations become increasingly difficult (converge slowly or even diverge) as the ratio of convection to diffusion increases. To overcome this problem, a multigrid approach is used in our study. Various applications of multigrid techniques to fluid-flow problems can be found in the literature [11–14].

In the present study, combined conduction and natural convection heat transfer modes have been analysed for an enclosure in three dimensions with heat generating components over substrates which are mounted horizantally and vertically. Fluid flow is driven by buoyancy forces and no additional pressure gradient is implemented. Effects of different parameters such as Rayleigh number, Prandtl number, heat source values of different magnitudes, on the temperature and flow fields are studied. Operator splitting is performed at three different levels: componentwise splitting results in the linearization of the differential/difference equations, except for the velocity term, for which we perform the second level of splitting. Directional splitting further simplifies the difference equations.

## 2. Mathematical modelling

Conservation of mass, momentum and energy equations are solved to determine the velocity components, pressure and temperature distributions inside an enclosure.

The energy equation is coupled with the Navier–Stokes equations, but it is quasi-linear; the convective terms involve products of unknown variables, i.e. components of the velocity vector and the temperature gradients.

Momentum equations of the Navier–Stokes model, however, are nonlinear. The acceleration terms involve products of the velocity vector and the columns of the velocity gradient tensor. We define two different "kinds" of velocities to overcome the nonlinearity in the momentum equations. That is one example of splitting, the second level mentioned above that we utilize in our model. "Dynamic" velocity components are computed at the centres of the control volume cells, similar to the unknown, i.e. temperature, of the energy equation, while

"kinematic" velocity components are defined at the walls of the control volume. Hence, the left-hand sides of the Navier–Stokes equations are linearized and take a form similar to that of the energy equation. The unknown velocity vector in the material derivative operator of the convective/acceleration terms, referred to as the "kinematic" velocity, is now treated separately, split from the velocity vector or momentum per unit mass, i.e. the unknown variable of the Navier–Stokes equation. An additional constraint is included in the analysis, which requires the equivalence of the solutions for the "kinematic" and "dynamic" velocities.

Subscripts identify the splitting as the velocity components appear in the differential equations given below. The governing equations in three-dimensional Cartesian coordinates, at steady state, in dimensionless form become as follows:
Continuity Equation:

$$\frac{\partial U_d}{\partial X} + \frac{\partial V_d}{\partial Y} + \frac{\partial W_d}{\partial Z} = 0 \tag{1}$$

X-momentum:

$$\frac{\partial (U_k U_d)}{\partial X} + \frac{\partial (V_k U_d)}{\partial Y} + \frac{\partial (W_k U_d)}{\partial Z} = -\frac{\partial P}{\partial X} + Pr\left(\frac{\partial^2 U_d}{\partial X^2} + \frac{\partial^2 U_d}{\partial Y^2} + \frac{\partial^2 U_d}{\partial Z^2}\right) \tag{2}$$

Y-momentum, with the Boussinesq approximation for the buoyancy term:

$$\frac{\partial (U_k V_d)}{\partial X} + \frac{\partial (V_k V_d)}{\partial Y} + \frac{\partial (W_k V_d)}{\partial Z} = -\frac{\partial P}{\partial Y} + Pr\left(\frac{\partial^2 V_d}{\partial X^2} + \frac{\partial^2 V_d}{\partial Y^2} + \frac{\partial^2 V_d}{\partial Z^2}\right) + Pr\,Ra\theta \tag{3}$$

Z-momentum:

$$\frac{\partial (U_k W_d)}{\partial X} + \frac{\partial (V_k W_d)}{\partial Y} + \frac{\partial (W_k W_d)}{\partial Z} = -\frac{\partial P}{\partial Z} + Pr\left(\frac{\partial^2 W_d}{\partial X^2} + \frac{\partial^2 W_d}{\partial Y^2} + \frac{\partial^2 W_d}{\partial Z^2}\right) \tag{4}$$

Energy:

$$\frac{\partial (U_k \theta)}{\partial X} + \frac{\partial (V_k \theta)}{\partial Y} + \frac{\partial (W_k \theta)}{\partial Z} = \left(\frac{\partial^2 \theta}{\partial X^2} + \frac{\partial^2 \theta}{\partial Y^2} + \frac{\partial^2 \theta}{\partial Z^2}\right). \tag{5}$$

For the volumetric heat-generating conducting solid body, the energy equation becomes

$$\left(k_s \frac{\partial^2 \theta}{\partial X^2}\right) + \left(k_s \frac{\partial^2 \theta}{\partial Y^2}\right) + \left(k_s \frac{\partial^2 \theta}{\partial Z^2}\right) = S \tag{6}$$

where the dimensionless variables are

$$\begin{aligned}
X &= \frac{x}{L} \quad U = \frac{u}{(\alpha/L)} \quad \theta = \frac{(T - T_c)}{\Delta T} \quad \Delta T = \frac{q''' H}{k_f} \\
Y &= \frac{y}{L} \quad V = \frac{v}{(\alpha/L)} \quad P = \frac{p}{\rho(\alpha/H)^2} \quad Pr = \frac{\nu}{\alpha} \\
Z &= \frac{z}{L} \quad W = \frac{w}{(\alpha/L)} \quad S = \frac{q''' H}{k_f \Delta T} \quad Ra = \frac{g\beta \Delta T H^3}{\nu\alpha}.
\end{aligned} \tag{7}$$

Two different types of boundary conditions are used in this study. In one of them (BC 1) all six walls are isothermal, and in the other (BC 2) five walls are insulated but only top wall is isothermal.

## 3. Solution procedure

In order to obtain a computational solution to the partial differential equations of the fluid motion, first these equations must be converted to algebraic equations. The finite volume method is used as the discretization procedure. The Picard method is used to resolve the coupling between momentum and energy equations. This can be viewed as a componentwise splitting. With the exception of velocity components, the Picard method eliminates nonlinearity. Each velocity component is further split into two, as dynamic and kinematic components, as explained above. Since the equations are now quasi-linear, convective/acceleration terms involve products of the unknown variables of different equations due to the coupling between the equations, but no products of an unknown variable with itself or its derivatives. The iterations are arranged according to the SIMPLE algorithm [15] by Patankar and Spalding [16].

After discretization and linearization of the governing equations, a directional splitting technique, ADI, namely Alternating Direction Implicit, is used to solve the system of equations. This method further splits each equation in the system of equations into three sets of equations, which can then be solved in sequence. In each sweep, we solve the equation in one particular direction, while the derivatives in the other two directions, those representing velocity and pressure gradients, are treated as known values, and appear as source terms. Following the splitting of the system of equations, the ADI method utilizes a tri-block-diagonal solver.

The Picard method is an iterative method. In this study we have eight unknowns, $U_d$, $V_d$, $W_d$, $U_k$, $V_k$, $W_k$, pressure and temperature, with five governing equations, which are the continuity equation, three momentum equations and the energy equation. Dynamic and kinematic velocity components that are computed separately at the centre and walls of the control volume, respectively, are equated using an averaging scheme: at the next iteration, at each grid point and for each velocity component, the average of the "dynamic"and "kinematic"values is used as the initial guess.

It is clear that momentum equations are for velocity components and temperature is solved by the energy equation. Since pressure does not appear in the continuity equation, we have to make some algebraic calculations for pressure correction.

When we discretize x-, y- and z-momentum equations we get,

$$\begin{aligned} a_P u_P &= \sum a_{nb} u_{nb} + (p_w - p_p) A_u + b_{uP} \\ a_P v_P &= \sum a_{nb} v_{nb} + (p_s - p_p) A_v + b_{vP} \\ a_P w_P &= \sum a_{nb} w_{nb} + (p_b - p_p) A_w + b_{wP} \end{aligned} \tag{8}$$

where $a_P$'s are the coefficients of the velocity components at a grid point P. Variable subscript $nb$ is used for points in the neighbourhood of the control volume, centred at P. After the discretization process, we obtain the above linear combination of the velocity components at point P and at the neighbouring points. Hence, $a_{nb}$'s are the coefficients of the velocity components at grid points in the neighbouring cells. The specific values of $a_P$ and $a_{nb}$ are dependent on the choice of discretization scheme. We use an upwind scheme for the first-order derivatives, and a central scheme for the second-order derivatives.

$A_u$, $A_v$ and $A_w$ are the cell face areas perpendicular to the velocity components $u$, $v$ and $w$ respectively.

$b_{*P}$s are the source terms, which arise from the energy equation coupling in the $y$-momentum equation, for an internal point P, or from the effects of boundary conditions for a boundary point P.

We first solve the above set of equations and name them as approximations $p^*$, $u^*$, $v^*$, $w^*$, to pressure and velocity components respectively. Each equation is linear and is solved using

an iterative linear solver, namely ADI. The explicit application of the method assumes that the coefficients $a_P$ and $a_{nb}$ values are constant for this initial solve to obtain the approximations $p^*$, $u^*$, $v^*$, $w^*$, even though these coefficients may depend on $p$, $u$, $v$, $w$. However, since we have split the "kinematic" variables from these unknown variables, our system is linear. Hence, the Picard method is applied implicitly.

One can define the pressure and velocity corrections $p'$, $u'$, $v'$ and $w'$, respectively, as the difference between their exact and approximate values, to get

$$\begin{aligned} a_P u'_P &= \sum a_{nb} u'_{nb} + (p'_w - p'_p) A_u \\ a_P v'_P &= \sum a_{nb} v'_{nb} + (p'_s - p'_p) A_v \\ a_P w'_P &= \sum a_{nb} w'_{nb} + (p'_b - p'_p) A_w. \end{aligned} \tag{9}$$

Omission of the $\sum a_{nb} u'_{nb}$, $\sum a_{nb} v'_{nb}$ and $\sum a_{nb} w'_{nb}$ terms is the main approximation of the SIMPLE algorithm [15].

$$\begin{aligned} u_P &= u^*_P + \frac{A_u}{a_P}(p'_w - p'_p) \\ v_P &= v^*_P + \frac{A_v}{a_P}(p'_s - p'_p) \\ w_P &= w^*_P + \frac{A_w}{a_P}(p'_b - p'_p). \end{aligned} \tag{10}$$

This is for a grid point P. We can easily write down similar relations for the neighbouring grid points; E (east), W (west), N (north), S (south), T (top) and B (bottom). Substitution of the corrected velocities of equations into the discretized continuity equation gives

$$\begin{aligned} &A_u\{[u^*_E + d_E(p'_P - p'_E)] - [u^*_W + d_W(p'_W - p'_P)])\} \\ &\quad + A_v\{[v^*_N + d_N(p'_P - p'_N)] - [v^*_S + d_S(p'_S - p'_P)]\} \\ &\quad + A_w\{[w^*_T + d_T(p'_P - p'_T)] - [w^*_B + d_B(p'_B - p'_P)]\} = 0 \end{aligned} \tag{11}$$

where

$$d_i = \frac{A_j}{a_i}. \tag{12}$$

Here the index $i$ stands for the grid location and the index $j$ for the velocity component. To solve for the pressure correction, first we have to solve the momentum equations, since $d$ terms

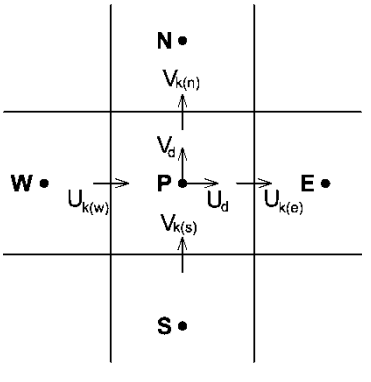


Figure 1. A typical finite volume cell with split velocity representation (2-D version).

in the pressure equation contain the velocity components. With new values for $u^*$,$v^*$ and $w^*$, the pressure can now be solved. The pressure correction equation is susceptible to divergence unless some under-relaxation is used during the iterative process and new, improved, pressure $p^{new}$ values are obtained with

$$p^{new} = p^* + \alpha_p p' \tag{13}$$

where $\alpha_p$ is the pressure under-relaxation factor. The velocities are also under-relaxed. The iteratively improved values are obtained from

$$\begin{aligned} u^{new} &= \alpha_u u + (1 - \alpha_u) u^{old} \\ v^{new} &= \alpha_v v + (1 - \alpha_v) v^{old} \\ w^{new} &= \alpha_w w + (1 - \alpha_w) w^{old}. \end{aligned} \tag{14}$$

$u^{old}$, $v^{old}$ and $w^{old}$ are velocity component values taken from the previous iteration. After the new values are computed, convergence must be checked.

Our system of discretized differential equations forms a heptadiagonal Jacobian matrix. Utilizing a directional splitting technique can surpass the difficulty of solving this heptadiagonal matrix. In this study, ADI (Alternating Direction Implicit) is used. The main idea behind this method is the splitting of this heptadiagonal matrix into a set of tridiagonal matrices [17], which are processed sequentially. This representation is Seidel-like. For a parallel implementation one should prefer a Jacobi-like representation.

## 4. Results and discussion

### 4.1 *Effects of physical parameters*

The Prandtl number $Pr$ is the ratio of the momentum and thermal diffusivities. It provides a measure of the relative effectiveness of momentum to energy transport by diffusion, in the velocity and thermal boundary layers, respectively. This means that when $Pr$ increases, momentum diffusivity is dominant to thermal diffusivity. Decrease of thermal diffusivity affects the thermal profile, making it non-toroidal. The Pr number affects the maximum temperature, $T_{\max}$, in the domain, significantly. Madhavan and Sastri [8] state that the fluid which has a $Pr = 25$ is the most suitable choice for this cooling problem because it has the minimum $T_{\max}$.

The $V$-component is the most dominant one within all of the velocity components and represents the primary upward fluid motion in the enclosure. However the value of $V$-component is very low at the bottom region, which means that the fluid is practically stagnant there. Increasing the Rayleigh number increases the vertical velocity, since the fluid is driven by the buoyancy force.

As the Rayleigh number increases, maximum temperature decreases. That is expected since heat transfer from the component to the fluid increases with increasing Rayleigh number. The transition to convective regime occurs in the range of $Ra$ from $10^3$ to $10^5$. At low Rayleigh numbers, an imbalance between the superposed effects of conduction and convection is reflected in a slow approach to the convective regime. The transition ends at $Ra = 10^5$. Increasing $Ra$ also increases the buoyancy effect and an increase in the buoyancy effect results in a decrease in the temperature gradient inside the enclosure and reduces the maximum temperature value over the component surface significantly. It is to be expected that, as the Rayleigh number increases, convection may become stronger and the convective heat transfer becomes more

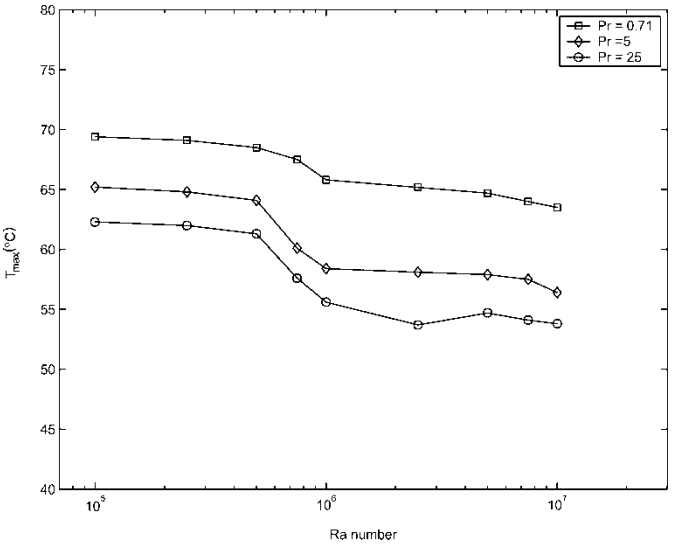


Figure 2. Variation of $T_{\max}$ with Rayleigh number for different Prandtl numbers.

important. This means that the heat is mostly conveyed by the dominating convection. At high Rayleigh numbers and at all boundary conditions, heat dissipated from the component cannot affect the fluid below the component. In this region ambient temperature does not change. The reason for this is the high cooling capacity of the upper enclosure wall. Especially at high Rayleigh numbers, the upper wall, when subjected to ambient temperature, is capable of removing heat dissipated from the component. In figure 2, the effects of different Rayleigh numbers with different Prandtl numbers on $T_{\max}$ can easily be seen.

### 4.2 *Effects of boundary conditions*

We have two different types of boundary conditions; in one case, all walls are at the ambient temperature, and in the other, only the top wall is at that temperature while the rest are insulated. The primary objective, keeping in mind the practical constraints, is to maintain the component temperature as low as possible by maintaining simple boundary conditions for the enclosure walls. The best way to maintain the temperature at a minimum level is to have isothermal conditions along its enclosure walls. This in turn would result in higher maintenance or cooling cost [8]. In order to be cost effective, however, all the walls, except the top wall where the gradients are high, are to be maintained at adiabatic conditions.

Fluid flow in the enclosure mainly consists of two circulating cells. The primary circulation is the result of the buoyancy force acting on the fluid. The secondary cell is a result of a combination of the splitting of fluid flow at the upper enclosure wall and heat transfer from the fluid to the enclosure wall containing the heat source. However, the chance of the formation of the secondary cell is weak, due to the insulation of the left wall. The $T_{\max}$ for BC 1 is less than for BC 2 due to to the increased heat transfer area of the enclosure walls.

### 4.3 *Multigrid implementation*

Some iteration methods like Jacobi and Gauss–Seidel are called “smoothers"since high frequency parts of the error (with respect to the stepsize of the grid) are reduced very rapidly,

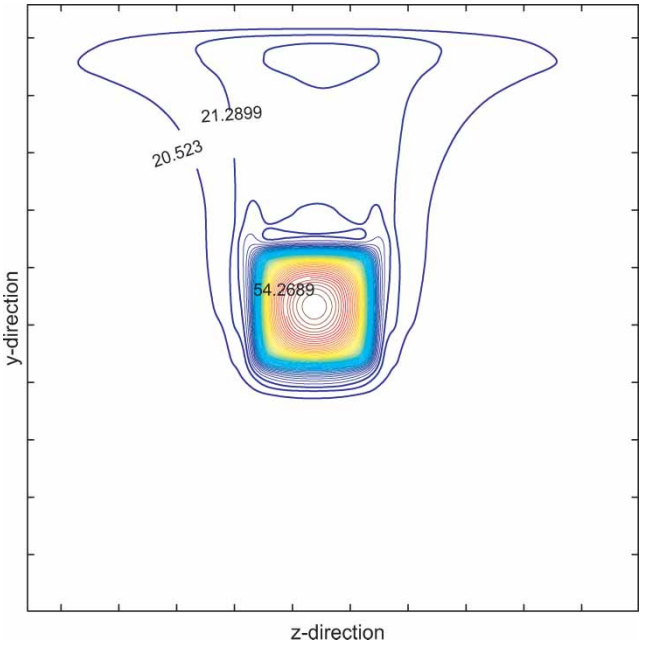


Figure 3. Isotherms (side view) at $Pr = 25$ and $Ra = 10^6$ with BC 1.

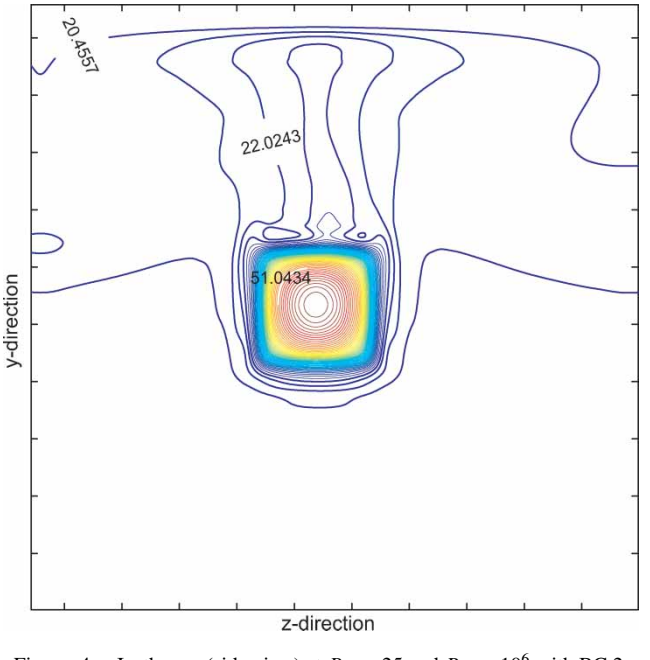


Figure 4. Isotherms (side view) at $Pr = 25$ and $Ra = 10^6$ with BC 2.

whereas low frequency error is reduced much more slowly. Thus, after a few iterations, we get a still quite big, but very smooth error. Instead of these methods, when multigrid is used, smooth errors can be represented well on a coarser grid, and on a coarser grid the error is less smooth with respect to the step size of the grid and can thus be reduced faster by a smoother on

this grid than on the original fine grid. In this present study when the single domain solution is used, the convergence rate deteriorates as the number of iterations increases. However, with the help of the multigrid method, with a coarse grid correction process to eliminate smooth errors, the convergence rate improves when the number of iterations increases, as shown in figure 7. In the multigrid code, a three-level V-cycle is used.

It is important to note that the main goal of the paper is to study operator splitting techniques at various levels, to formulate an efficient method for convection–diffusion operators. Multi-grid implementation is included here just to improve the convergence characteristics. We do not intend to emphasize the use of multi-grid techniques in relation to operator splitting. On the other hand, multi-grid/level techniques are very effective in solving systems of differential equations, whether they are applied to Newton- or Picard-linearized nonlinear equations or directly used as nonlinear solvers, for example, FAS (Full Approximation Scheme). Equation-wise splitting may still be useful then, if one uses either decoupled or distributive relaxations. For the case of distributive relaxation, decoupled relaxation follows a suitable transformation [18].

## 5. Concluding remarks

A numerical study has been performed to observe the effects of Rayleigh number, Prandtl number and boundary conditions on the solution of natural convection heat transfer from one or multiple heat sources mounted horizontally or vertically on substrates within enclosures. To speed up the rate of convergence some splitting techniques are implemented at every step of the solution.

One type of splitting operation in this study is to differentiate between the velocity variables, according to the way it appears in the governing equations. They are named dynamic and

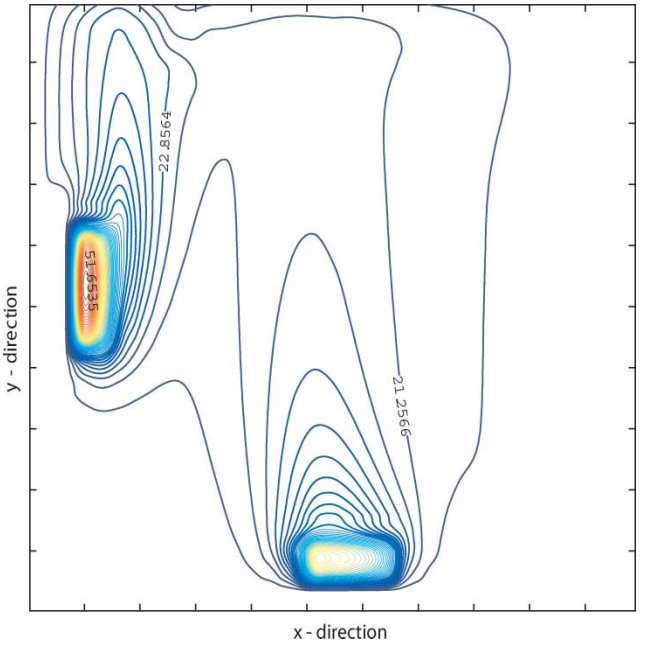


Figure 5. Isotherms of two chips at $Pr = 5$ and $Ra = 10^6$ with BC 1.

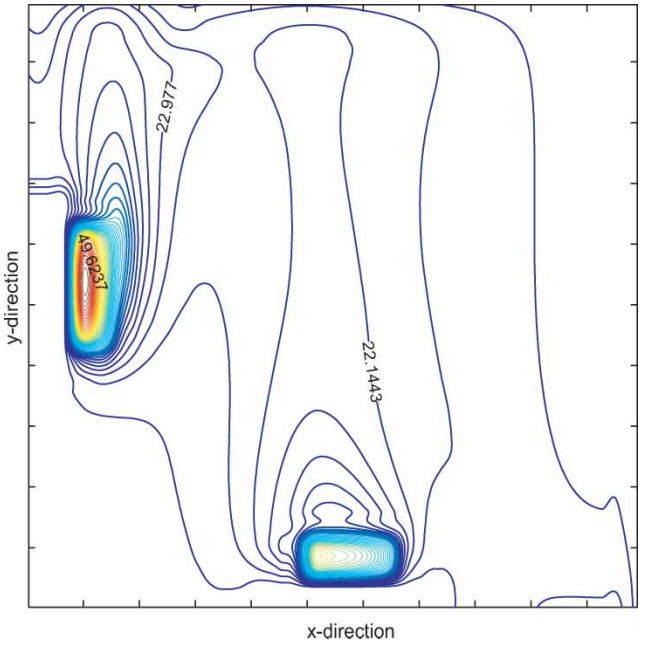


Figure 6. Isotherms of two chips at $Pr = 5$ and $Ra = 10^6$ with BC 2.

kinematic velocities. The former is defined at the centre of the control volume and the latter is defined at the wall of the control volume. Another splitting is componentwise, known as the Picard Method. It resolves the coupling between pressure and velocities. Another splitting applied in this study is directional splitting, know as the Alternating Direction Implicit (ADI) method. Hence, the linear system of algebraic equations obtained through the Picard method is solved by the ADI Method. The main characteristic of this method is to split the system into three sweep directions, which are the generalized coordinates directions. After splitting

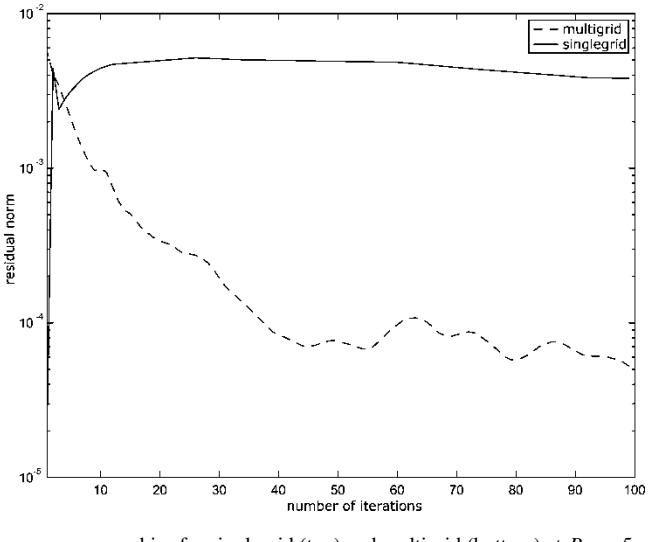


Figure 7. Convergence graphics for singlegrid (top) and multigrid (bottom) at $Pr = 5$ and $Ra = 10^5$.

heptadiagonal matrices into tridiagonal matrices, these tridiagonal matrices can be solved easily by tridiagonal matrix solvers.

A multigrid method has been used to increase the convergence rate by eliminating smooth errors. A V-cycle method has been used in the multigrid algorithm. The first coarser grid calculation is used as a preconditioner and the second one to eliminate smooth errors.

At the end of this study some physical results have been obtained for the model problem. These are: (1) heat transfer and fluid flow are strongly affected by Rayleigh number and boundary conditions; (2) $T_{\max}$ is affected especially by the Prandtl number; (3) convection heat transfer mode plays a more significant role in the heat transfer inside the enclosure when the Rayleigh number starts to increase; (4) using a multigrid reduces the residual norms significantly.

## Acknowledgements

This work was funded by a grant from Bogazici University Research Fund, BAP no. 02A601.

## References

[1] Heindel, T.J., Ramadhyani, S. and Incropera, F.P., 1995, Conjugate natural convection from an array of discrete heat sources: part 1 Two- and three-dimensional model validation. *International Journal of Heat and Fluid Flow*, **16**(6), 501–510.

[2] Ha, M.Y. and Jung, M.J., 2000, A numerical study on three-dimensional conjugate heat transfer of natural convection and conduction in a differentially heated cubic enclosure with a heat-generating cubic conducting body. *International Journal of Heat and Mass Transfer*, **43**, 4229–4248.

[3] Deng, Q.H., Tang, G.F. and Li, Y., 2002, A combined temperature scale for analyzing natural convection in rectangular enclosures with discrete wall heat sources. *International Journal of Heat and Mass Transfer*, **45**, 3437–3446.

[4] Deng, Q.H., Tang, G.F., Li, Y. and Ha, M.Y., 2002, Interaction between discrete heat sources in horizontal natural convection enclosures. *International Journal of Heat and Mass Transfer*, **45**, 5117–5132.

[5] Kehoe, E., Davies, M. and Newport, D., 2003, Mixed convection cooling of horizontally mounted printed circuit board. *IEEE Transactions on Components and Packaging Technologies*, **26**, 126–133.

[6] Eveloy, V. and Rodgers. P., 2004, Numerical prediction of electronic component operational temperature: A perspective. *IEEE Transactions on Components and Packaging Technologies*, **27**, 268–282.

[7] Eveloy, V. and Rodgers. P., 2005, Prediction of electronic component-board transient conjugate heat transfer. *IEEE Transactions on Components and Packaging Technologies*, **28**, 817–829.

[8] Madhavan, P.N. and Sastri V.M.K., 2000, Conjugate natural convection cooling of protruding heat sources mounted on a substrate placed inside an enclosure: a parametric study. *Computer Methods in Applied Mechanics and Engineering*, **188**, 187–202.

[9] Sezai, I. and Mohamad A.A., 2000, Natural convection from a discrete heat source on the bottom of a horizontal enclosure. *International Journal of Heat and Mass Transfer*, **43**, 2257–2266.

[10] Dağtekin, I. and Öztop, H.F., 2001, Natural convection heat transfer by heated partitions within enclosure. *International Communications in Heat and Mass Transfer*, **28**(6), 823–834.

[11] Karki, K.C., Sathyamurthy, P.S. and Patankar, S.V., 1996, Performance of a multigrid method with an improved discretization scheme for three-dimensional fluid flow calculations. *Numerical Heat Transfer Part B*, **29**, 275–288.

[12] Thompson, M.C. and Ferziger, J.H., 1989, An adaptive multigrid technique for the incompressible Navier–Stokes equations. *Journal of Computational Physics*, **82**, 94–121.

[13] Vincent, S. and Caltagirone, J.P., 2000, Numerical solving of incompressible Navier–Stokes equations using an original local multigrid refinement method. *Comptes Rendus de l'Academie des Sciences Series IIB Mechanics Physics Astronomy*, **328**(1), 73–80.

[14] Montero, R.S., Llorente, I.M. and Salas, M.D., 2001, Robust multigrid algorithms for the Navier–Stokes equations. *Journal of Computational Physics*, **173**, 412-432.

[15] Versteeg, H.K. and Malalasekera, W., 1995, *An Introduction to Computational Fluid Dynamics* (London: Prentice Hall).

[16] Patankar, S.V., 1980, *Numerical Heat Transfer and Fluid Flow* (New York: Hemisphere Publishing Corporation).

[17] Hoffmann, K.A. and Chiang, S.T., 1993, *Computational Fluid Dynamics For Engineers*, Vol. 1 (Kansas: Engineering Education System).

[18] Trottenberg, U., Oosterlee, C. and Schueller, A., 2001, *Multigrid* (London: Academic Press).